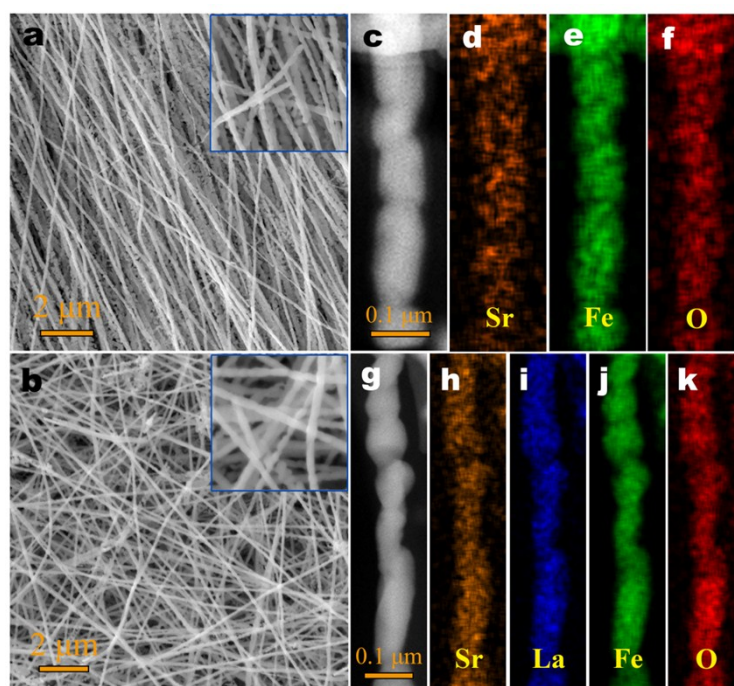


## Supporting Information

### Direct imaging of dopant sites in rare-earth-element-doped permanent magnet and correlated magnetism origin

Xue Zeng,<sup>†a</sup> Junwei Zhang,<sup>†a</sup>, Mingsu Si,<sup>a</sup> Derang Cao,<sup>c</sup> Xia Deng,<sup>a</sup> Hongbin Ma,<sup>d</sup>

Qianqian Lan,<sup>a</sup> Desheng Xue,<sup>a</sup> Xixiang Zhang,<sup>\*b</sup> Kun Tao<sup>\*a</sup> and Yong Peng<sup>\*a</sup>



**Fig. S1 Morphological characterisation of the M-type SFO and SLFO single-particle-chain nanofibres. (a-b)** Low-magnified SEM image. Inset, magnified SEM image showing that the nanofibres morphologically consist of single nanoparticles stacked along the nanofibre axis. **(c)** Representative HAADF-STEM image of a single SFO single-particle-chain nanofibre. **(d-f)** EDX elemental mappings of

strontium, iron and oxygen. (g) HAADF-STEM image of another single SLFO single-particle-chain nanofibre. (h-k) Elemental mappings of strontium, lanthanum, iron and oxygen.

Quantitative analysis shows that their average length is approximately 120  $\mu\text{m}$  and average diameter is approximately 80 nm ranging from 70-100 nm. Energy-dispersive X-ray spectroscopy (EDX) and elemental mappings showed a 1:12 atomic ratio of Sr:Fe for SFO nanofibres, inferring a  $\text{SrFe}_{12}\text{O}_{19}$  chemical composition.

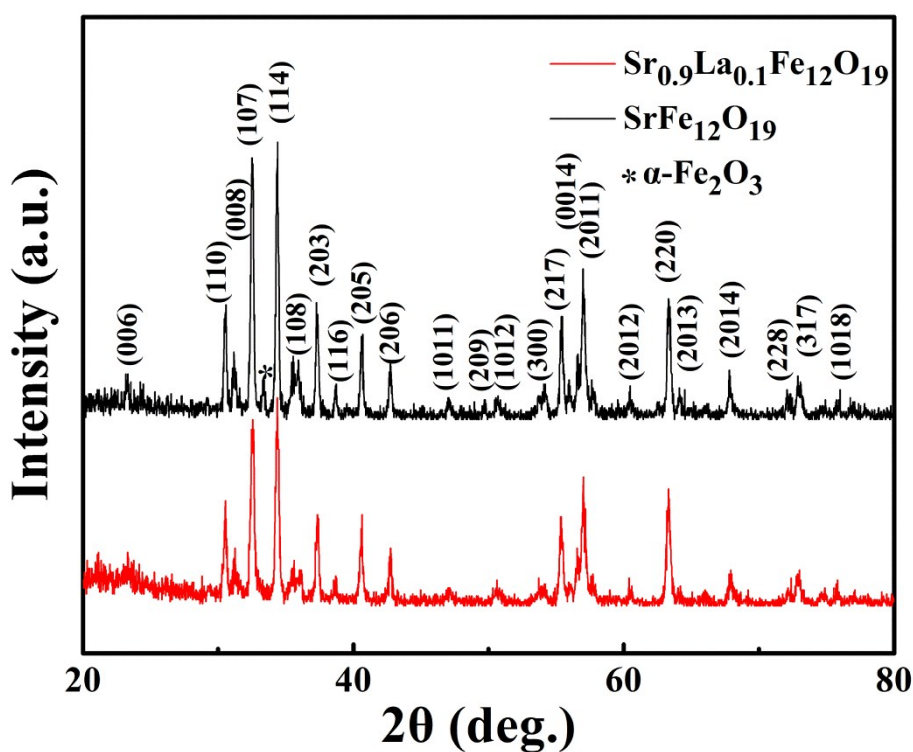


**Fig. S2 XRD spectra of the  $\text{SrFe}_{12}\text{O}_{19}$  and  $\text{Sr}_{0.9}\text{La}_{0.1}\text{Fe}_{12}\text{O}_{19}$  nanofibres.**

Both spectra show that their peaks can be indexed to (006), (110), (008), (107), (114), (108), (203), (116), (205), (206), (1011), (209), (1012), (300), (217), (0014), (2011), (2012), (220), (2013), (2014), (228), (317),

and (1018) planes, indicating a magnetoplumbite structure. This result is consistent with the crystal characterisation observed by using TEM.

The main peaks of the red spectrum (SLFO) in Fig. S3 correspond to the hexagonal M-type phase (SrM JCPDS Card no. 27–1029), revealing that the La atoms have been successfully doped into the SFO and formed a single phase SLFO without intermediate phases. XRD analysis points that the diffraction peak position for  $\text{La}^{3+}$  doped ferrite exactly appears at same position as for  $x=0$ . The spectra also show a little bit presence of secondary ( $\alpha\text{-Fe}_2\text{O}_3$ ) phase in SFO pattern and are disappeared after La-doping. The  $\alpha\text{-Fe}_2\text{O}_3$  phase should originate from the incomplete reaction between  $\text{Fe}^{3+}$  and  $\text{Sr}^{2+}$  or low solubility of  $\text{Sr}^{2+}$  in primary SFO nanofibre in comparison with the La-doped specimen.

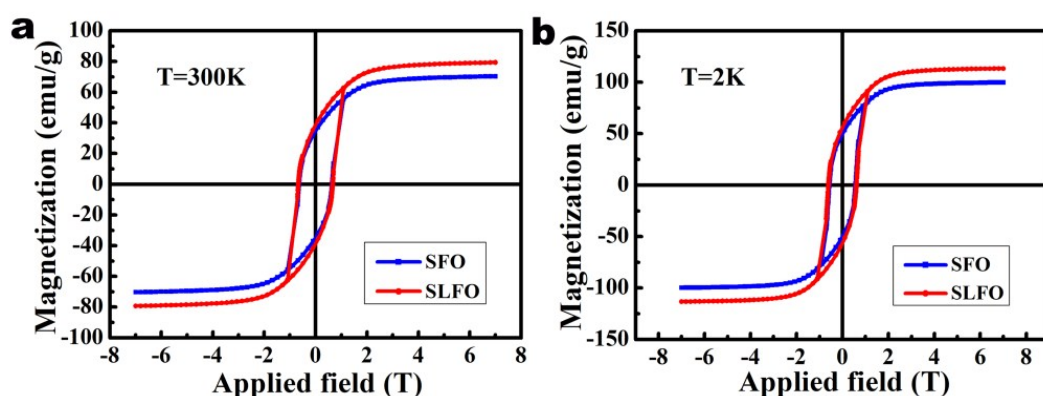


**Fig. S3 Magnetic properties of the SFO and SLFO single-particle-chain nanofibres.** (a-b) Magnetic-field dependence of magnetization measured at 300 K and 2 K.

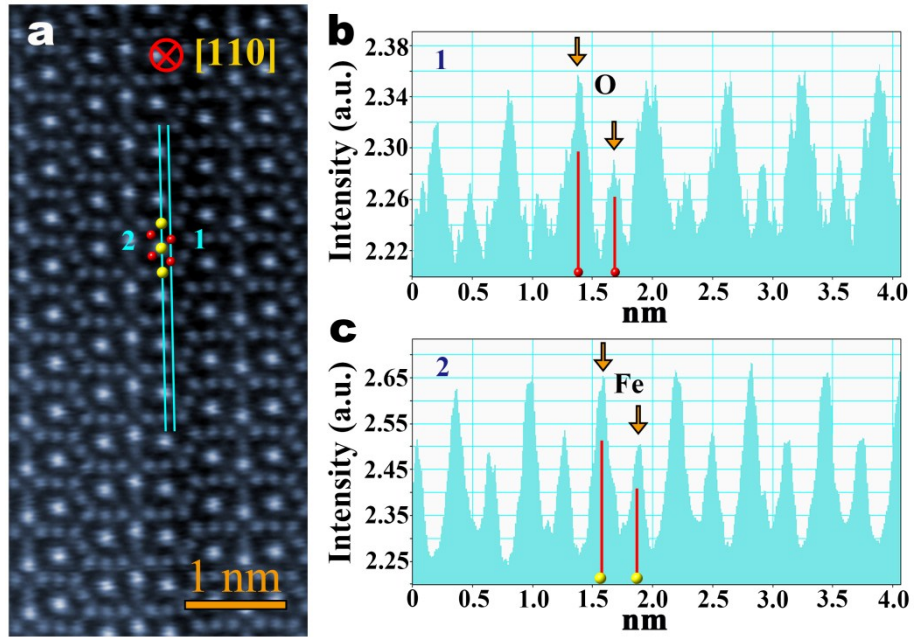


**Fig. S4 Ionic position and ordering analysis of the M-type SFO nanofibres.** (a) The experimental HAADF-STEM images of the SFO nanofibres projected along [110] orientation. (b-c) Line intensity profiles of blue lines “1” and “2” in (a) showing the position and ordering of O and Fe atom columns. The intensity variations at the different sites are not constant due to the number of atoms in each particular atom column.

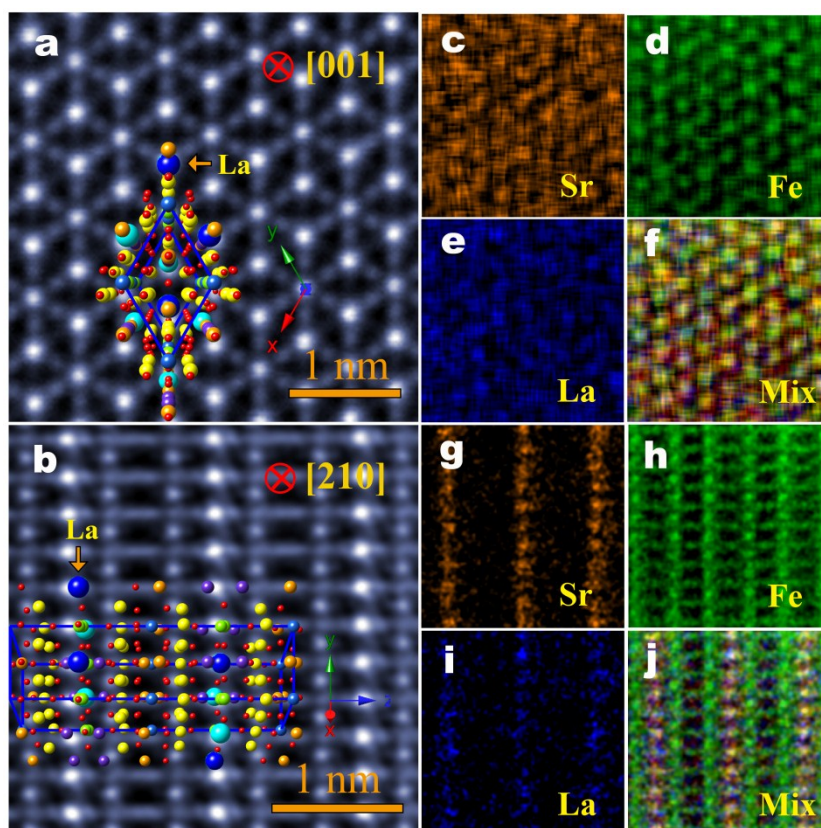


**Fig. S5 La-cations substitutional analysis of the  $\text{Sr}_{0.9}\text{La}_{0.1}\text{Fe}_{12}\text{O}_{19}$  nanofibres.** (a-b) HAADF-STEM images under [001] and [210] orientations. (c-f) and (g-j) Their corresponding EDX atomic-scale elemental mappings of Sr, Fe, La and mixed columns, respectively.

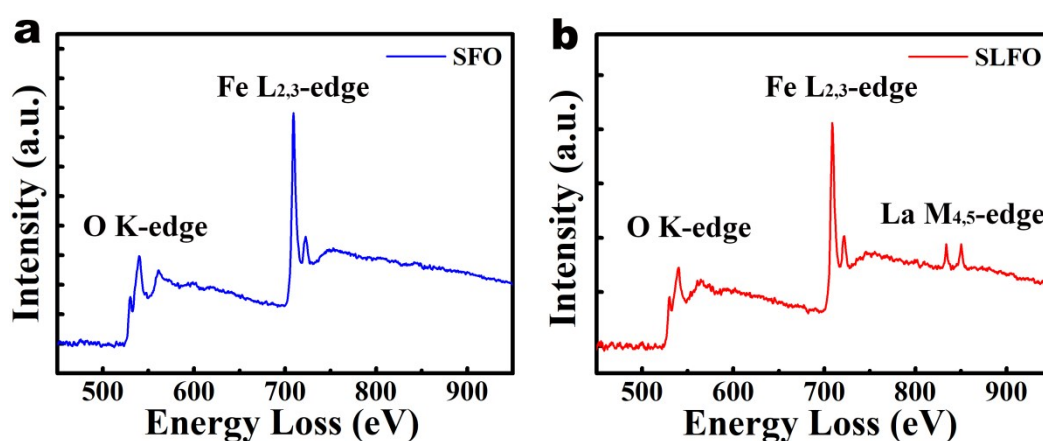


**Fig. S6 Dual EELS spectrum characterisation.** (a-b) Measured EELS full spectrum in large region, depicting the valence states of SFO and SLFO.



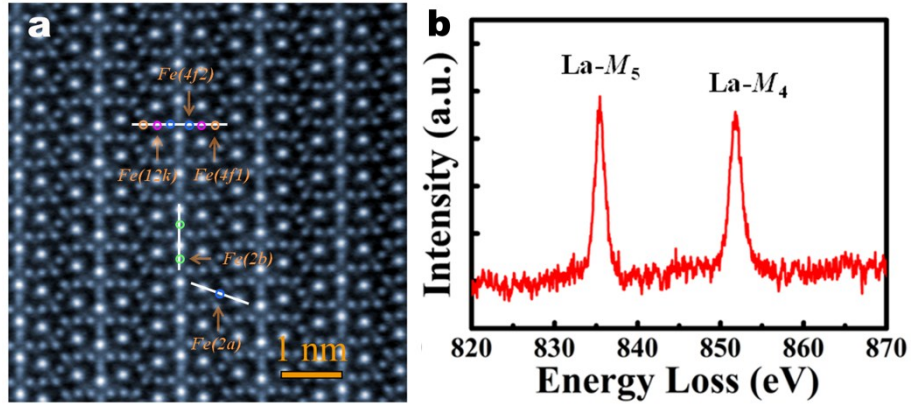


**Fig. S7 Valence state characterisation of the SLFO nanofibres.** (a) atomic resolution STEM image under [011] orientation, where the white lines show the scanning positions. (b) La  $M_{4,5}$ -edge average EELS spectra of the SLFO nanofibres detected from about 15 atomic columns, which shows the oxidation state of the La ions is 3+, which coincides well with the standard La EELS spectrum in EELS Atlas.

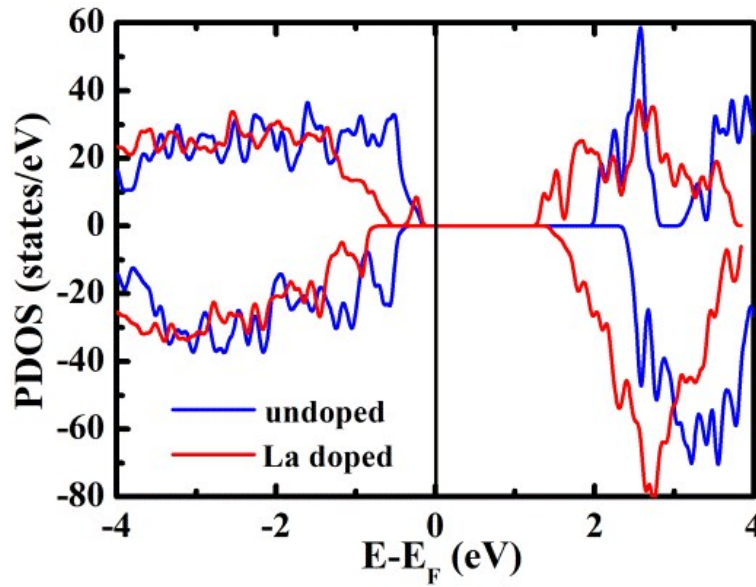


**Fig. S8 Density functional theory calculations.** DOS for SFO and SLFO near the Fermi energy level.

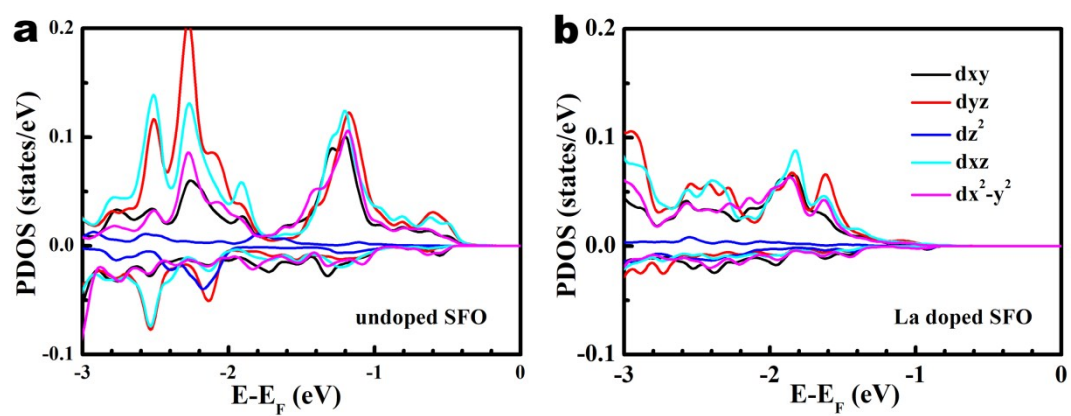


**Fig. S9 Density functional theory calculations. (a-b)** d orbitals of Fe9 (at 2a site) atoms with different energy levels of SFO and SLFO.